PHYSICAL REVIEW A VOLUME 39, NUMBER 8 APRIL 15, 1989

# Correlation in double electron capture in collisions of fully stripped ions on He and $H_2$

M. Mack,* J. H. Nijland, P. v. d. Straten,† and A. Niehaus
*Fysisch Laboratorium, Rijksuniversiteit te Utrecht, Princetonplein 5, NL-3584 CC Utrecht, Utrecht, The Netherlands*

R. Morgenstern
*Kernfysisch Versneller Instituut, Rijksuniversiteit te Groningen, Zernikelaan 25, NL-9747 AA Groningen, Groningen, The Netherlands*

(Received 2 June 1988; revised manuscript received 6 September 1988)

Energy spectra of electrons resulting from collisions of bare ions $C^{6+}+H_2$ and $O^{8+}+He$ are presented. A detailed analysis is given for those parts of the spectra that are due to two-electron capture into $(3l,3l')$ configurations of the He-like projectile ions and subsequent autoionization. Measured peaks are uniquely identified by comparison with existing theoretical calculations. Based on a detailed investigation, it is concluded that an influence of interference effects on the spectra cannot be identified. A quantitative fit of the spectra allows us to determine the population probabilities of the various states with $(3l,3l')$ configuration. We find a preferential population of states that can be characterized by a correlated electronic motion with the two electrons on opposite sides of the capturing ion and rotating in the same sense. This result is discussed in terms of a classical picture for the capturing process.

## I. INTRODUCTION

It is well known that an independent electron model is insufficient to describe various quantities such as energies and lifetimes of states with two or more electrons. Correlation has to be taken into account for a good quantitative description, especially for electrons with the same principal quantum number. On the other hand, it is unclear how far electron correlation has an influence on dynamical processes, such as charge exchange or excitation, and there has recently been some discussion[1,2] with respect to this. A two-electron system consisting of a fully stripped ion like $C^{6+}$ or $O^{8+}$ and a two-electron target like He or $H_2$ is well suited to study this question: Electrons are mainly captured into excited states, and capture of both electrons leads to a population of doubly excited states, which subsequently decay by electron emission in an autoionization process. Analysis of the electron energy spectra allows us to find out how far certain classes of doubly excited correlated states are populated when both electrons are transferred from the target to the projectile ion. One could, e.g., suspect that those states are preferred, in which both electrons are "on the same side" of the ion, since they are both transferred from a well-localized area, i.e., their initial separation within the target is small as compared with the most relevant impact parameters. As will be seen in the following, such a suspicion is not justified. First, experimental results on the population of the correlated states of the $(3l,3l')$ configuration have recently been obtained by Bordenave-Montesquieu *et al.*[3] for the $N^{7+}+He$ system, and by Mack and Niehaus[4] for the system $O^{8+}+He$ and $C^{6+}+H_2$. An analysis of the data on the $N^{7+}+He$ system in terms of a quantitative fit, yielding numbers for the population probabilities of the various states, is included in Ref. 3. In the procedure that was applied the possibility of the influence of interference of overlapping contributions from different states was not discussed. In this paper we present an analysis on the data of the $O^{8+}+He$ and $C^{6+}+H_2$ systems. The spectra are measured at an electron emission angle of $\vartheta=50°$. As opposed to $\vartheta=10°$—used in Ref. 3 for the $N^{7+}+He$ system—one expects a larger Doppler broadening of measured peaks. Nevertheless, we observe well-resolved peaks even at places where only broad structures have been observed in Ref. 3 for $N^{7+}+He$. Therefore we regard the quantitative fits of our spectra as being more critical than those of Ref. 3, especially as they allow us to investigate the following questions.

(i) Are there certain classes of correlated states that are preferably excited?

(ii) Is it allowed, for our case of noncoincident measurements, to neglect interferences between autoionizing transitions?

(iii) Which of the theoretically determined energies and lifetimes for the various states, presented in Tables I and II, are most dependable?

## II. EXPERIMENT

The experimental setup has been outlined in Ref. 5 and in detail in Ref. 6 and is only briefly described here. A schematic drawing for our apparatus is shown in Fig. 1. Fully stripped ions $C^{6+}$ and $O^{8+}$ are produced in an electron cyclotron resonance (ECR) ion source of the MINIMAFIOS type[7] which is installed at the Kernfysisch Versneller Instituut (KVI) in Groningen.[8] Behind the first deflection magnet respective beam

 

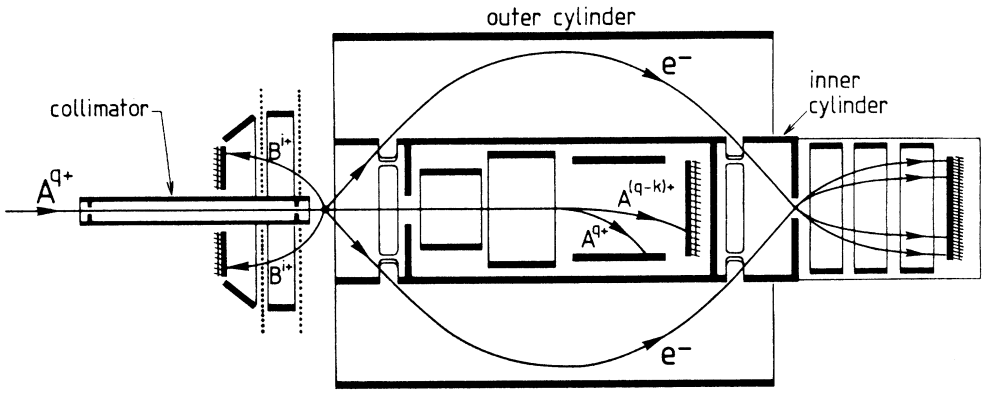


FIG. 1. Schematic view of the apparatus. For the experiments described here only the electron analyzer part has been used.

currents of 0.3 and $\sim 0.1$ $\mu$A are obtained. Before entering the scattering chamber the ion beam is collimated by two diaphragms of 1 mm diameter at 50 mm distance. For the reaction center we estimate a beam diameter of less than 1.5 mm and a beam divergence of $\sim 7$ mrad. Some percent of the above-mentioned currents arrive at this place. The energy spread of the ions after having passed the various focusing elements and switching magnets is estimated to be less than 2 eV.

The target gas enters the reaction center through a ring-shaped conical channel (4.5 mm long, 0.2 mm wide) that forms an angle of 63.5° with the electron spectrometer axis and which points to the reaction center. The channel ends in a ring slit with a diameter of 14 mm at a distance of 3.5 mm from the reaction center. The tip of the cone defined by the gas inlet channel coincides with the "viewing point" of the electron spectrometer and forms the reaction center. This gas inlet system resulted in a considerable increase of the target gas density in the reaction center (a factor of 8.4±0.5 with respect to the residual gas was measured for He and $H_2$). To insure single collision conditions the background gas pressure was kept below $5\times10^{-8}$ mbars for all measurements.

The electron spectrometer is a cylindrical mirror analyzer (CMA) with radii for the inner and outer cylinder of 56±0.03 and 142.85±0.03 mm, respectively, and a distance of focal points of $z_0=376.9\pm0.1$ mm. It has an acceptance angle with respect to the ion beam direction of $\vartheta_e=50°\pm2.4°$, a calculated energy resolution of $\Delta E/E=3\times10^{-2}$ and an estimated solid angle detection fraction of $\leq 1\times10^{-2}$. Its design is based on the trajectory calculation for finite source size of Draper and Lee.[9] The whole spectrometer is surrounded by a triple $\mu$-metal shielding which reduces the external fields (1–3 G from the KVI cyclotron magnet) by a factor of $\sim 1000$. The spectrometer is operated in a constant-$\Delta E/E$ mode, i.e., the transmission energy is varied by scanning the voltage $U_c$ on the outer cylinder. The corresponding number of detected electrons is counted by means of a channel-plate detector and stored in a multichannel analyzer, the channels of which are switched synchronously with the stepwise variation of $U_c$. The electron spectra shown in the following have been corrected for the energy-dependent spectrometer transmission by multiplying all channel contents by a factor proportional to $(E_{\rm lab})^{-1}$. Also a correction factor of $(E_{\rm em}/E_{\rm lab})^{1/2}$ has been applied in order to obtain electron intensities in the emitter frame[10] ($E_{\rm em}$ and $E_{\rm lab}$ are electron energies in the emitter and laboratory frame, respectively).

## III. EXPERIMENTAL RESULTS

Figures 2 and 3 show in an overview energy spectra of electrons resulting from $^{13}C^{6+}+H_2$ collisions and $^{18}O^{18+}+He$ collisions at energies of 60 and 96 keV, respectively. Since we look for possible effects of correlation we are mainly interested in the electrons between 20 and 30 eV for the $C^{6+}+H_2$ case and between 30 and 40 eV for the $O^{8+}+H_2$ case since these are due to autoionization from doubly excited states with the configuration $(3l,3l')$, i.e., with equal principal quantum numbers for

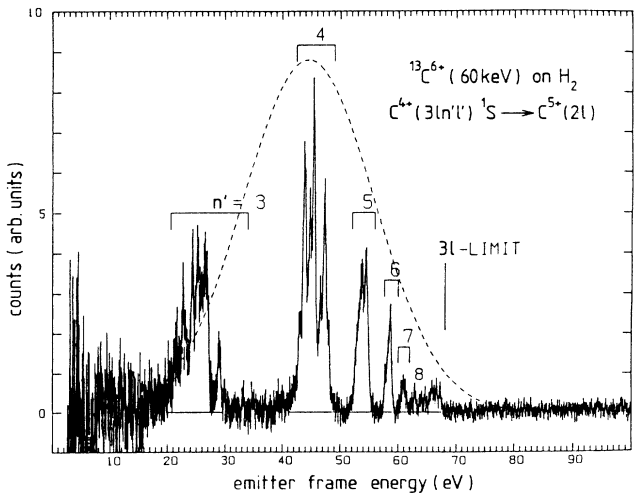


FIG. 2. Energy spectrum of electrons from $^{13}C^{6+}+H_2$ collisions at 60 keV. The energy scale refers to the electron emitter frame. The dashed line indicates the reaction window as calculated from the extended classical barrier model (Ref. 11).

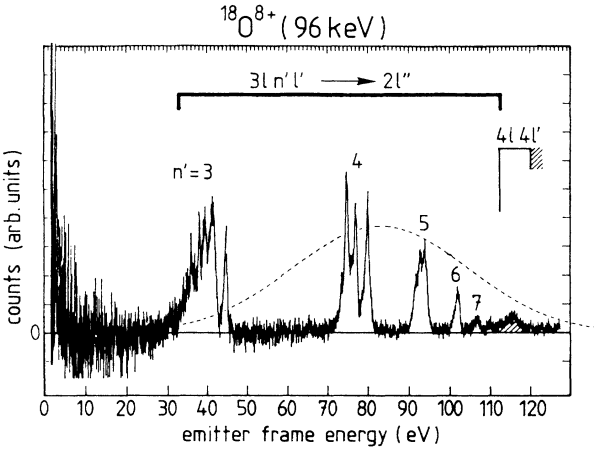


FIG. 3. Energy spectrum of electrons from $^{18}O^{8+}+He$ collisions at 96 keV. The energy scale refers to the electron emitter frame. The dashed line indicates the reaction window as calculated from the extended classical barrier model (Ref. 11).

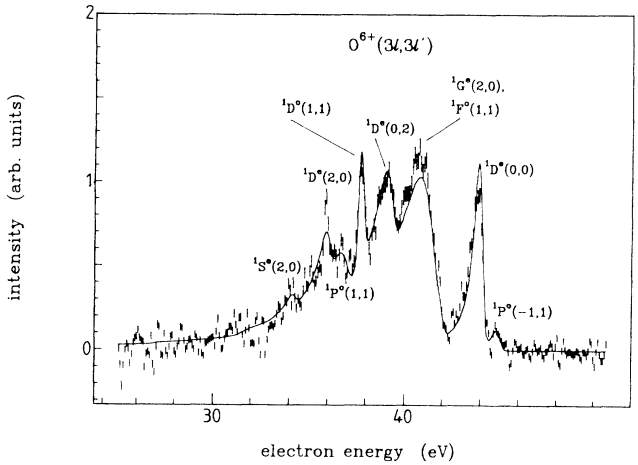


FIG. 5. Part of the spectrum of Fig. 3 showing electrons from autoionizing $O^{6+}$ states with $(3l,3l')$ configuration. Identification of states is according to the calculations of Ho (Refs. 21 and 22). The approximate correlation quantum numbers $(K,T)$ are indicated for a characterization of states.

both electrons, giving rise to the most pronounced correlation effects. Therefore these groups of electron peaks are shown separately in Figs. 4 and 5, respectively. First of all, it should be noted that a broadening of the peaks due to kinematical effects apparently does not play an important role. The narrowest peaks have a width of $\delta\varepsilon=300$ meV. A kinematical broadening could be produced by an uncertainty of electron detection angles with respect to the direction of the electron emitted projectiles and is given by

$$\delta\varepsilon \approx 4\left[\frac{m}{M}\varepsilon_e E\right]^{1/2} \sin\vartheta_e(\Delta\vartheta_e+\theta_p)\ , \tag{1}$$

with $m$ and $M$ the masses of electron and emitting ion, respectively. The term $\theta_p$ is caused by the velocity components perpendicular to the beam direction which are distributed with equal probabilities over all azimuthal angles $\phi$. For our conditions ($\vartheta_e=50°$, $\varepsilon_e\approx 30$ eV, and $E=60$ or 96 keV, respectively) one finds that $\Delta\vartheta_e+\theta_p\le 1°$. At first glance this result seems to be in contradiction to the fact that the uncertainty $\Delta\vartheta$ of the detection angle (caused by the spectrometer slit width) is 2.4°. However, the influence of $\Delta\vartheta$ on $\Delta\varepsilon$ is in reality smaller than implied by Eq. (1) since the kinematical energy shift of the electrons, connected with different emission angles, is partly compensated by the focusing properties of the spectrometer. As is discussed in more detail in Ref. 6, electrons at angles smaller than the nominal detection angle of $\vartheta_e=50°$ need a somewhat larger energy than those at 50° in order to be focused to the same point. The degree of compensation between Doppler shift and focusing properties is different for different electron and projectile energies. However, for the parts of the spectra to be discussed in the following there is a very good compensation. We estimate that $\theta_p<0.5°$, which means that the overwhelming majority of electrons is due to processes corresponding to a small deflection of the projectile. The main reason for this is the fact that electron capture predominantly occurs at large impact parameters. This is well understood in terms of the modified classical overbarrier model[11] and will be exploited in the discussion of possible interference effects.

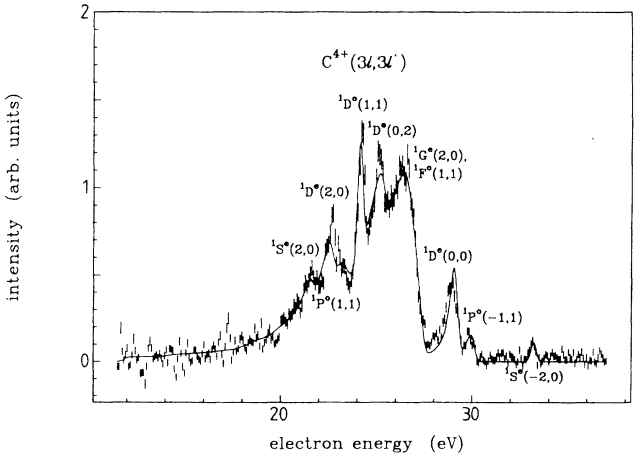


FIG. 4. Part of the spectrum of Fig. 2, showing electrons from autoionizing $C^{4+}$ states with $(3l,3l')$ configuration. Identification of states is according to the calculations of Ho (Refs. 21 and 22). The approximate correlation quantum numbers $(K,T)$ are indicated for a characterization of states.

## IV. ANALYSIS OF THE SPECTRA

### A. Autoionizing states, contributing to the spectra

Figures 4 and 5 show those parts of the energy spectra in which the electrons are due to autoionization from states with the configuration $(3l,3l')$. For the interpretation of the spectra we take only singlet states into account since the electrons have been captured from He and $H_2$ where the electrons initially have opposite spin.

A spin change is very unlikely, as was discussed by Mack.[12] Besides their total spin, angular momentum, and parity, the states are also characterized by their correlation quantum number $(K,T)^A$ as, e.g., discussed by Lin.[13] In our case these latter quantum numbers are especially interesting since they give an indication about the different types of correlated electron motion in the various states. $K=2$, e.g., indicates that the electrons are predominantly on opposite sides of the nucleus and $T=0$ indicates a preferential motion of both electrons in the same plane. The quantum number $A$ characterizes the radial correlation. In our case, where both electrons have the same principle quantum number $n=3$, it is always $A=+1$ and therefore no longer specified in the following.

Theoretical calculations for the energies and lifetimes of autoionizing states have been performed by various methods. Lipsky *et al.*[14] and Bachau[15,3] calculated position and width of quasibound states within a scattering continuum by means of a Feshbach formalism. A variational close-coupling method has been used to determine doubly excited states as resonances in the electron scattering cross section of hydrogenic ions for $C^{4+}$ and $O^{6+}$ by Abu-Salbi and Callaway and for $N^{5+}$ by Oza.[17,18] Ho[19–22] applied a complex coordinate rotation method and determined width and position of doubly excited states from complex eigenvalues of the Hamiltonian. Martin *et al.*,[23] finally, calculated $N^{5+}$ states using a variant of the Feshbach method, based on the addition of a pseudopotential to the Hamiltonian. The various calculations are in qualitative agreement in the sense that they all lead to the same identification of the various peaks, which is indicated in Figs. 4 and 5. There are, on the other hand, significant differences in the predicted values of energies and widths, and a comparison with our spectra will allow us to get information on the dependability of the various types of calculations. Also, since our spectra exhibit well-resolved peaks, it will be possible to determine the contributions of various states to the spectra quantitatively. For this, however, a detailed analysis of the spectra is essential.

### B. Spectral shapes and intensities

A quantitative analysis of noncoincident electron energy spectra has been performed earlier by v.d. Straten *et al.*[24] and also by Wada *et al.*[25] In principle the spectral distribution of ejected electrons can for a well-defined scattering event be described by

$$\frac{d\sigma(\theta_p)}{d\mathbf{k}}=2\pi\left|\sum_{L,M} f(\varepsilon_L,\varepsilon)a_{LM}(\theta_p)Y_{LM}(\mathbf{k})\frac{\langle k'L,\beta_f 0;L\|V_A\|\beta_\rho L\rangle}{\sqrt{2L+1}}\right|^2, \tag{2}$$

[For a short derivation of (2) see, e.g., Eq. (5) of Ref. 26.] Here $a_{LM}$ are the complex population amplitudes for the various magnetic sublevels $M$ of the states $L$, the $Y_{LM}$ are spherical harmonics, and $\langle\cdots\|V_A\|\cdots\rangle$ are reduced matrix elements for autoionization, essentially given by the lifetime of the doubly excited states. The $f(\varepsilon_L,\varepsilon)$ are the so-called post-collision-interaction (PCI) amplitudes, the squares of which describe the energy distribution of electrons from a single state. For a decay of an isolated atom the $f(\varepsilon_L,\varepsilon)$ represent a Lorentzian at the energy $\varepsilon_L$. However, due to the PCI—i.e., the Coulomb interaction between the emitted electron and the slowly receding, ionized collision partner—the line is shifted and becomes asymmetric. The $f(\varepsilon_L,\varepsilon)$ have to be modified accordingly. For the simplest case (where the collision velocity $V$ is small as compared to the electron velocity $v_0$ and therefore the internuclear separation of the collision partners can be regarded as constant during the electron emission process), Barker and Berry[27] derived a line shift which to a good approximation is given by $-Q/2V\tau$ with $Q$ the charge of the PCI-inducing collision partner and $\tau$ the lifetime of the decaying state. For higher velocities $V$ both the PCI shift and the peak shape become emission angle dependent, as was discussed by v.d. Straten and Morgenstern[28] and by Arcuni.[29] In our analysis we use PCI amplitudes $f(\varepsilon_L,\varepsilon)$ as given by v.d. Straten and Morgenstern,[30] which yield peak maxima at a position which is shifted by

$$\Delta\varepsilon=-\frac{Q}{2V\tau}\left[1-\frac{V}{|\mathbf{V}-\mathbf{v}_0|}\right]. \tag{3}$$

Quite understandably this shift of the measured peak with respect to the theoretical positions deviates from the normal PCI shift $-Q/2V\tau$ especially for the case $\mathbf{V}-\mathbf{v}_0=0$, i.e., when the emitted electron and the PCI-inducing collision partner are moving with equal velocities in the same direction. The shift according to (3) is taken into account in the peak identifications of Figs. 4 and 5.

In Eq. (2) the sum of amplitudes is squared and this implies that interferences can occur between various autoionization amplitudes. Such interferences have in fact been observed[26,31,32] as pronounced structures in energy spectra of electrons, measured in coincidence with scattered projectiles, i.e., for well-defined collision events.

Noncoincident spectra, however, can be regarded as an incoherent superposition of coincident ones. Such a superposition could wash out the interference structures and it is questionable if they are observable at all, or if they can just be neglected in the analysis of the spectra. In the following we discuss this question in some detail since it turns out that in the case of the processes investigated here, an influence of interferences can by no means be excluded *a priori*.

One can distinguish four different effects which will lead to a smoothing of interference structures.

(i) Kinematical shifts are different for spectra corresponding to a well-defined scattering angle $\Theta_P$ of the projectile but to different azimuthal orientations $\Phi$ of the scattering plane.

(ii) Kinematical shifts are different for spectra corresponding to different scattering angles $\Theta_P$ of the projectile.

(iii) The interference structures themselves will be different for spectra corresponding to different orientations of the scattering plane.

(iv) Interference structures may be different for different $\Theta_p$ since the phases of the population amplitudes $a_{LM}$ may depend on the scattering angle.

One can easily see that (i) and (ii) can in our case not lead to a complete extinguishing of interference structures: from the theoretical understanding of the charge exchange process one knows that only a narrow range of small scattering angles—corresponding to large impact parameters—is responsible for the overwhelming fraction of electrons. One can estimate that shifts of the spectra due to different orientations of the scattering plane are smaller than 0.1 eV. This is supported by the sharpness of the observed structures which were discussed in Sec. III.

The influence of (iii) can be treated in an analytical way if one assumes that energy shifts caused by (i) and (ii) are negligible with respect to the natural linewidth: then the total spectral electron intensity is given by an integral of (2) over all azimuth angles $\phi$ and scattering angles $\Theta_p$ of the projectile

$$\frac{d\sigma}{d\varepsilon\, d\vartheta}=\int_0^{2\pi}d\phi\int_0^{\pi}d\Theta_p\frac{d\sigma(\theta_p)}{d\mathbf{k}}\sin\theta_p\ . \tag{4}$$

The integration over the azimuth angles $\phi$ can be done by using the relation

$$\int Y_{LM}(\Omega)Y^*_{L'M'}(\Omega)d\phi=\tfrac{1}{2}(-1)^M\delta_{MM'}\sum_J(2J+1)\sqrt{(2L+1)(2L'+1)}\begin{bmatrix}L & L' & J\\ 0 & 0 & 0\end{bmatrix}\begin{bmatrix}L & L' & J\\ M & -M & 0\end{bmatrix}P_J(\cos\vartheta)\ . \tag{5}$$

This integration removes all interferences between levels with different magnetic quantum numbers $M$.

In order to take (iv) into account we have to perform an integration over all scattering angles $\theta_p$. For this we introduce the averaged quantities $\tilde{\rho}_{LML'M}$ given by

$$\tilde{\rho}_{LML'M}=\int a_{LM}(\theta_p)a^*_{L'M}(\theta_p)\sin\theta_p d\theta_p\ . \tag{6}$$

This yields an averaged cross section for electron emission given by

$$\frac{d\bar{\sigma}}{d\varepsilon\, d\vartheta}=\sum_{L,L'}C_{LL'}(\vartheta)\langle L\|V_a\|L\rangle\langle L'\|V_a\|L'\rangle^*\times f(\varepsilon_L,\varepsilon)f^*(\varepsilon_{L'},\varepsilon)\ , \tag{7}$$

where the coefficients $C_{LL'}$ are given by

$$C_{LL'}(\vartheta)=\tfrac{1}{2}\sum_{J,M}(-1)^M\tilde{\rho}_{LML'M}(2J+1)\begin{bmatrix}L & L' & J\\ 0 & 0 & 0\end{bmatrix}\times\begin{bmatrix}L & L' & J\\ M & -M & 0\end{bmatrix}P_J(\cos\vartheta)\ . \tag{8}$$

In Eq. (8) the terms containing $C_{LL'}$ with $L\neq L'$ describe interferences of autoionizing transitions from different states and the question is, how large are their contributions relative to the $C_{LL}$ terms? This is to a large extent determined by the ratio

$$\lambda^2=\tilde{\rho}^2_{LML'M}/(\tilde{\rho}_{LMLM}\tilde{\rho}_{L'M'L'M'})\ , \tag{9}$$

with $0\le\lambda^2\le 1$. The interference terms will be small if contributions to the population of $L,M$ sublevels are due to a large range of scattering angles $\theta_p$ and if at the same time the phases of $a_{LM}$ and $a_{L'M}$ vary differently as functions of $\theta_p$. However, as we have discussed above, collisions leading to a small range of scattering angles are responsible for most of the electrons. Therefore the resulting phase variation of the corresponding $a_{LM}$ is small and one can suspect that the $\lambda$ values are close to 1.

### C. Fit procedures

In order to see how far it is important or necessary to take interferences of autoionizing transitions from different states into account in the interpretation of the spectra we followed different fit procedures.

(i) "Incoherent fits," in which only intensities of electrons from different autoionization states are superimposed. The spectral intensity is essentially given by

$$I(\vartheta,\varepsilon)=\sum_L|f_L(\varepsilon)|^2\,|A_L(\vartheta)|^2\ , \tag{10}$$

where the $A_L$ contain the population amplitudes $a_{LM}$ multiplied by the spherical harmonics $Y_{LM}$ and the reduced matrix elements.

(ii) "Coherent fits," in which also interferences are taken into account. Here the proper procedure would be to take the $C_{LL'}$ of Eq. (8) as fit parameters. This would automatically take care of excluding interferences between transitions from levels with different $M$. With $N=11$ states possibly contributing to the spectra shown in Figs. 4 and 5, however, this would result in $\frac{1}{2}N(N+1)=66$ fit parameters. We regard this as too much and therefore followed a simpler though less accurate procedure. We used the following expression for the spectral intensity:

$$I(\vartheta,\varepsilon)=\sum_L|f_L(\varepsilon)|^2|A_L(\vartheta)|^2+\sum_{L\neq L'}|f_L(\varepsilon)|\,|f_{L'}(\varepsilon)|\,|A_L(\vartheta)|\,|A_{L'}(\vartheta)|\cos[\alpha_L(\varepsilon)-\alpha_{L'}(\varepsilon)+\beta_L(\vartheta)-\beta_{L'}(\vartheta)]\ , \tag{11}$$

with $\alpha_L(\varepsilon)=\arg[f_L(\varepsilon)]$ and $\beta_L(\vartheta)=\arg[A_L(\vartheta)]$. The moduli $|A_L|$ and the phases $\beta_L$ were taken as fit parameters. In this way we have reduced the number of fit parameters to 22. However, one has to keep in mind that in this way certainly "too many interferences" are taken into account, since also those between amplitudes from levels with different $M$ are included. One can in fact suspect that reality lies between (i) and (ii).

(iii) "Fits with selected interferences," in which physical insight is used to take only those interference terms into account which can be expected to have the most significant influence on the spectra. Interferences between states lying close to each other are certainly more important than those between states far apart from each other. Also the lifetime of the higher states is of importance: states with short lifetimes result in peak shapes with intensive low-energy tails, corresponding to large transition amplitudes at the position of the lower states. The most visible effects can therefore be expected from interferences of transitions from the strongly populated and short-lived states $^1G$ and $^1F$ (see Figs. 4 and 5) with those from lower states. To further limit the number of free parameters one can argue that especially strong interferences can be expected for the case of transitions leading to similar angular electron distributions. Since the angular electron distributions are closely connected with the electron density distributions[26] and these on their part are to a large extent characterized by the correlation quantum numbers (for $T=0$, e.g., both electrons are in the same plane), we expect that interferences between states with the same $(K,T)$ values are most likely to produce a visible effect in the spectra. We therefore looked specifically for such interferences.

We started with incoherent fits, assuming in the first place fixed positions $\varepsilon_L$ and widths $\Gamma_L$ of the contributing states as given by theory, and only taking the population amplitudes as fit parameters. For most of the sets $(\varepsilon_L,\Gamma_L)$ this resulted in unsatisfactory fits which could significantly be improved by changing the $(\varepsilon_L,\Gamma_L)$ values. Only the theoretical results of Abu-Salbi and Callaway[16] and the most recent results from Ho led immediately to rather good fits. We took this as a strong indication of the correctness of the corresponding $(\varepsilon_L,\Gamma_L)$ values.

In a second step we tried to improve these fits by performing coherent fits as described above. This did not result in a significantly improved agreement, neither did it lead to drastically different populations of the various states as compared to the incoherent fits. Since, on the other hand, it is possible, just by choosing phases arbitrarily, to create significant disagreement with the measured spectra, we take this as an indication that interferences are not of an overwhelming importance.

In a third step we performed fits with selected interferences. As a test whether or not the selection of a particular set of interferences would affect the fit we used the following general expression for the spectral intensity:

$$I(\vartheta,\varepsilon)=\sum_L |f_L(\varepsilon)|^2\,|A_L(\vartheta)|^2+\sum_{\substack{L,L'\\L\neq L'}} |f_L(\varepsilon)|\,|f_{L'}(\varepsilon)|\,|C_{LL'}(\vartheta)|\cos[\alpha_L(\varepsilon)-\alpha_{L'}(\varepsilon)-\gamma_{LL'}(\vartheta)]\ , \tag{12}$$

with $\gamma_{LL'}(\vartheta)=\arg[C_{LL'}(\vartheta)]$. We looked at the interferences between $^1F(1,1)$ and $^1D°(1,1)$ and between $^1G(2,0)$ and $^1D(2,0)$. These are interferences between states with the same $(K,T)$ which could appear on the prominent low-energy tail of the $^1F(1,1)$ and the $^1G(2,0)$ peaks, respectively. Also this did not lead to significantly improved fits.

### D. Fit results

For the incoherent fits with fixed energies and lifetimes of the states involved we used sets of data from various theoretical treatments. An overview of these data is given in Table I for $C^{4+}(3l,3l')$ and in Table II for $O^{6+}(3l,3l')$. The calculations had in some cases been performed for $N^{5+}(3l,3l')$ and in order to use these data we have extrapolated them for the case of $O^{6+}$ and $C^{4+}$ by the following procedure: the lifetimes were assumed to be independent of $Z$ and the term energies were assumed to vary with $Z$ according to

$$\varepsilon(nl,nl')=\left[\frac{Z-\alpha}{n}\right]^2\ , \tag{13}$$

with a screening constant $\alpha$ which is independent of $Z$, i.e., $\alpha$ is calculated from the energy values $\varepsilon(nl,nl')$ for the $N^{5+}$ system and then used to determine the analogous energy values for $O^{6+}$ and $C^{4+}$ states. Figure 4 shows a fit of the $C^{4+}$ spectrum using the theoretical $(\varepsilon,\Gamma)$ values of Ho.[21] Only the populations of the various states were used as fit parameters. It should be pointed out that the energies and widths from Ho[22] which are used in Fig. 4 are very similar to those obtained earlier by Abu-Salbi and Callaway (see Table I). The quality of our spectra is in fact not sufficient to discriminate between these two sets of data. On the other hand, we can clearly see that fits with the other data sets given in Table I lead to a less satisfactory agreement with the experimental spectra. Not only the energy positions of the states are probed by our fits, but also their widths; these are on the one hand directly reflected in the peak widths, and on the other have also an important influence on the actually measured peak positions since the PCI shift as given in Eq. (3) leads to a shift of the peak maxima by about $-3.5\Gamma$ for the case of $^{13}C$ (60 keV). The rather accurate prediction of lifetimes is especially remarkable since the lifetimes are very sensitive to electron correlations: the agreement therefore indicates that correlation effects in the stationary states are properly taken into account in the calculations of Abu-Salbi and Callaway and of Ho.

For the case of $O^{8+}+He$, fit results are shown in Fig. 5. In this case the use of fixed $(\varepsilon,\Gamma)$ sets from theory did not directly yield satisfactory results and therefore we al-

TABLE I. State energies (first lines) and width (second lines), both in eV, for $C^{4+}(3l,3l')$ states as predicted by various theoretical treatments. Energies are given with respect to the $n=2$ level of $C^{5+}$, i.e., the final state in the autoionization of $C^{4+}$ (Ref. 4). The last column gives the relative populations (in %) of the various states following from the fit shown in Fig. 4. An asterisk means that the energy values below were obtained by extrapolation using Eq. (13).

| States $^{2S+1}L$ $(K,T)$ | Ho (Ref. 22) | Ho (Ref. 19) | Bachau* (Ref. 3) | Bachau (Ref. 15) | Oza* (Ref. 18) | Martin* *et al.* (Ref. 23) | Abu-Salbi and Callaway (Ref. 16) | Population (%) |
|---|---|---|---|---|---|---|---|---|
| $^1S(2,0)$ | 21.42 | 21.42 | 21.54 | 21.45 | 21.43 | | 21.42 | 2 |
| | 0.130 | 0.129 | 0.170 | 0.166 | 0.139 | | 0.129 | |
| $^1D(2,0)$ | 22.51 | | 22.61 | 22.48 | 22.52 | | 22.51 | 6 |
| | 0.177 | | 0.230 | 0.233 | 0.180 | | 0.176 | |
| $^1P^0(1,1)$ | 23.39 | 23.40 | 23.56 | 23.43 | 23.43 | 23.28 | 23.41 | 3 |
| | 0.381 | 0.381 | 0.440 | 0.427 | 0.403 | 0.400 | 0.389 | |
| $^1D^0(1,1)$ | 23.82 | | 23.96 | | 23.85 | | | 5 |
| | 0.0084 | | 0.011 | | 0.0084 | | | |
| $^1D(0,2)$ | 25.31 | | 25.55 | 25.42 | 25.36 | | 25.32 | 12 |
| | 0.310 | | 0.350 | 0.338 | 0.327 | | 0.307 | |
| $^1S(0,0)$ | 25.51 | 25.51 | 25.75 | 25.61 | 25.61 | | 25.53 | |
| | 0.523 | 0.525 | 0.60 | 0.578 | 0.544 | | 0.524 | |
| $^1G(2,0)$ | 26.96 | | 27.29 | | 27.17 | | 26.99 | 55 |
| | 0.620 | | 0.770 | | 0.544 | | 0.639 | |
| $^1F^0(1,1)$ | 27.22 | | 27.65 | | 27.39 | | 27.26 | 8 |
| | 0.316 | | 0.380 | | 0.357 | | 0.327 | |
| $^1D(0,0)$ | 28.90 | | 29.39 | | 29.12 | | 28.98 | 6 |
| | 0.0789 | | 0.120 | | 0.117 | | 0.109 | |
| $^1P^0(-1,1)$ | 29.82 | 29.82 | 30.38 | 30.24 | 30.15 | 30.90 | 29.97 | 2 |
| | 0.106 | 0.106 | 0.110 | 0.107 | 0.114 | 0.113 | 0.110 | |
| $S(-2,0)$ | 32.88 | 32.88 | 33.49 | | | | | 1 |
| | 0.0078 | 0.0077 | 0.0064 | | | | | |

TABLE II. The same as Table I, but for $O^{6+}(3l,3l')$. In addition, state energies are given which result from the fit shown in Fig. 5, since none of the theoretical sets of energies gave satisfactory fit results.

| States | Ho (Ref. 22) | Ho (Ref. 19) | Bachau* (Ref. 3) | Bachau (Ref. 15) | Oza* (Ref. 18) | Martin* *et al.* (Ref. 23) | Abu-Salbi and Callaway (Ref. 16) | Expt. | Population (%) |
|---|---|---|---|---|---|---|---|---|---|
| $^1S(2,0)$ | 34.68 | 34.68 | 34.82 | 34.70 | 34.58 | | 34.68 | 34.80 | 1 |
| | 0.138 | 0.136 | 0.17 | 0.166 | 0.139 | | 0.136 | | |
| $^1D(2,0)$ | 36.15 | | 36.26 | 36.15 | 36.05 | | 36.15 | 36.69 | 4 |
| | 0.176 | | 0.230 | 0.233 | 0.180 | | 0.176 | | |
| $^1P^0(1,1)$ | 37.40 | 37.40 | 37.54 | 37.45 | 37.29 | 37.16 | 37.42 | 37.66 | 8 |
| | 0.381 | 0.381 | 0.440 | 0.427 | 0.403 | 0.400 | 0.389 | | |
| $^1D^0(1,1)$ | 37.94 | | 38.08 | | 37.84 | | | 38.19 | 3 |
| | 0.0084 | | 0.011 | | 0.0084 | | | | |
| $^1D(0,2)$ | 40.01 | | 40.23 | 40.15 | 39.89 | | 40.02 | 40.06 | 14 |
| | 0.329 | | 0.35 | 0.365 | 0.327 | | 0.340 | | |
| $^1S(0,0)$ | 40.36 | 40.36 | 40.50 | 40.47 | 40.22 | | 40.39 | | |
| | 0.569 | 0.569 | 0.60 | 0.621 | 0.544 | | 0.58 | | |
| $^1G(2,0)$ | 42.41 | | 42.59 | | 42.34 | | 42.45 | 42.21 | 48 |
| | 0.708 | | 0.77 | | 0.544 | | 0.735 | | |
| $^1F(1,1)$ | 42.82 | | 43.07 | | 42.63 | | 42.87 | 42.59 | 9 |
| | 0.362 | | 0.38 | | 0.357 | | 0.380 | | |
| $^1D(0,0)$ | 45.09 | | 45.44 | | 44.99 | | 44.23 | 44.51 | 12 |
| | 0.114 | | 0.12 | | 0.117 | | 0.122 | | |
| $^1P(-1,1)$ | 46.46 | 46.46 | 46.79 | 46.95 | 46.38 | 47.50 | 46.65 | 45.52 | 1 |
| | 0.118 | 0.118 | 0.11 | 0.118 | 0.114 | 0.113 | 0.121 | | |
| $^1S(-2,0)$ | 50.64 | 50.64 | 51.03 | | | | | | |
| | 0.069 | 0.069 | 0.064 | | | | | | |

lowed for a variation of the energy positions of the states involved. The widths, however, were not varied but we used the widths calculated by Ho[17] which are again very close to those calculated by Abu-Salbi and Callaway. In Table II we present various sets of theoretical $(\varepsilon,\Gamma)$ values together with the state energies following from our fit. At present it is not clear to us why in the case of $O^{6+}$ the experimentally determined energies differ significantly from all the theoretical ones, whereas this was not the case for $C^{4+}$. As in Table I we give again the relative populations of the various states following from our fit.

As in the case of $C^{4+}$ above we proceeded by performing coherent fits. However, this did again not significantly improve the fit results, nor did it lead to drastically different populations of the various states. The same is true for fits with selected interferences. We therefore take the population probabilities obtained from the incoherent fits as the basis for the discussion of the physics of the charge exchange process. Also we conclude that very probably the neglect of interferences in the analysis of $N^{5+}$ spectra by Bordenave-Montesquieu *et al.*[3] did not give rise to additional uncertainties of their results. However, it should be pointed out that the relative unimportance of interference effects could not dependably be predicted and therefore it was necessary to perform a corresponding analysis as presented above.

## V. DISCUSSION

In order to see if the population of certain configurations is preferred by the dynamics of the charge exchange process we can compare the observed populations with those to be expected statistically. As one can see from Table II our analysis shows that more than 50% of the electrons are ejected from the state $^1G(2,0)$. Statistically one would expect significantly less (only 20%), and it is worth speculating about a possible mechanism responsible for this. The correlation quantum numbers $(K,T)=(2,0)$ characterize states with both electrons moving in the same plane ($T=0$) on opposite sides of the nucleus ($K=2$),[13] and the angular momentum $L=4$ indicates that both electrons are rotating in the same sense. This implies the following picture for the capture of the two electrons: (i) the electrons are not simultaneously becoming "molecular" when the collision complex is formed, but with a time delay of at least one-half electron revolution time. (ii) The second electron behaves in a correlated way, namely, such that with respect to the first one it ends up on the opposite side of the quasimolecular orbit. Classically this can be understood by keeping in mind that the second electron experiences a time-dependent potential. At a fixed internuclear distance $R$ of the collision partners the Coulomb barrier, which has to be overcome by the second electron in order to become molecular, will change its height dependent on the position of the "first" electron. The lower barrier corresponding to the electron on the "other" side will then cause a preferential population of configurations with correlation quantum numbers $K=2$. (iii) The correlation within the quasimolecular formed during the collision is preserved in the electronic configuration of the projectile state when the collision partners separate.

We have performed some simple calculations in order to check if such a completely classical picture can have any significance. According to the extended classical barrier model[11] the internuclear distances in the $O^{8+}$ on He system, at which the first and second electron can be transferred, are $R_1=7.4$ a.u. and $R_2=5.0$ a.u., respectively. First of all, we checked if the transition of the second electron can really be regarded as localized in the sense that the probability for tunneling at internuclear distances between $R_1$ and $R_2$ can be regarded as small. Using WKB functions for the electron we found that with a probability of $\sim 70\%$ the second electron is still at the target atom—i.e., it has not yet made a transition—when the system reaches the distance $R_2$. At $R_2$ the transition probability suddenly becomes very large, provided that the first electron really does not cause any screening of the projectile charge $q$, as has been assumed in the calculation of $R_2$. On the other hand, if one assumes that, due to a position of the first electron on the "same" side, the second electron sees an effective charge $q-1$, an internuclear distance of $R_2'=4.7$ would have to be reached to allow an overbarrier transition. Keeping in mind that at $R_2$ the effective binding energy of the second electron is $\sim 5.6$ a.u. and that the projectile velocity is only 0.46 a.u., one can justify an adiabatic picture in which the transition of the second electron near $R_2$ is clearly preferred. This implies a preferential population of configurations with a correlation quantum number $K=2$—in agreement with the experimental observations. The same preferential population has been found in Ref. 3 for the case of $N^{7+}+He$ collisions.

We therefore conclude that electron correlation has a well-recognizable influence on the charge exchange process, in which two electrons are transferred from one collision partner to the other.

## ACKNOWLEDGMENTS

This work is a part of the research program of the Stichting voor Fundamenteel Onderzoek der Materie (FOM) with financial support from the Stichting voor Zuiver-Wetenschappelijk Onderzoek (ZWO).

*Also at Kernfysisch Versneller Instituut Groningen. Present address: Universität Dortmund, D-4600 Dortmund 50, Federal Republic of Germany.

†Present address: State University of New York at Stony Brook, Stony Brook, NY 11794.

[1]N. Stolterfoht, C. O. Havener, R. A. Phaneuf, J. K. Swenson, S. M. Shafroth, and F. W. Meyer, Phys. Rev. Lett. **57**, 74 (1986).

[2]H. Winter, M. Mack, R. Hoekstra, A. Niehaus, and F. J. de Heer, Phys. Rev. Lett. **58**, 957 (1987).

[3]A. Bordenave-Montesquieu, P. Benoit-Cattin, M. Boudjema, A. Gleizes, and H. Bachau, J. Phys. B **20**, L695 (1987).

[4]M. Mack and A. Niehaus, in *Abstracts of the Fifteenth International Conference on the Physics of Electronic and Atomic Collisions, Brighton, 1987,* edited by J. Geddes, H. B. Gilbody, A. E. Kingston, and C. J. Latimer (Queen's University, Belfast, 1987), p. 567.
[5]M. Mack and A. Niehaus, Nucl. Instrum. Methods B **23**, 291 (1987).
[6]M. Mack, Ph.D. thesis, Groningen, 1987 (unpublished).
[7]R. Geller and B. Jacquot, Nucl. Instrum. Methods **202**, 399 (1982).
[8]A. G. Drentje, Nucl. Instrum. Methods B **9**, 526 (1985).
[9]J. E. Draper and C-Y. Lee, Rev. Sci. Instrum. **48**, 852 (1977).
[10]P. Dahl, M. Rodbro, B. Fastrup, and M. E. Rudd, J. Phys. B **9**, 1567 (1976).
[11]A. Niehaus, J. Phys. B **19**, 2925 (1986).
[12]M. Mack, Nucl. Instrum. Methods **23**, 74 (1987).
[13]C. D. Lin, in *Invited Papers of the Fourteenth International Conference on the Physics of Electronic and Atomic Colisions, Palo Alto, 1985,* edited by D. C. Lorents, W. E. Meyerhof, and J. R. Peterson (North-Holland, Amsterdam, 1986), p. 643.
[14]L. Lipsky, R. Amania, and M. J. Coneely, At. Data Nucl. Data Tables **20**, 127 (1977).
[15]H. Bachau, J. Phys. B **17**, 1771 (1984).
[16]N. Abu-Salbi and J. Callaway, Phys. Rev. A **24**, 2372 (1981).
[17]D. H. Oza, Phys. Rev. A **33**, 824 (1986).
[18]D. H. Oza, J. Phys. B **20**, L13 (1987).
[19]Y. K. Ho, J. Phys. B **12**, 387 (1979).
[20]Y. K. Ho, Phys. Lett. **79A**, 44 (1980).
[21]Y. K. Ho, Phys. Rev. A **35**, 2035 (1987).
[22]Y. K. Ho (private communication).
[23]F. Martin, O. Mo, A. Riera, and M. Yanez, Europhys. Lett. **4**, 799 (1987).
[24]P. v.d. Straten, P. M. Koenraad, R. Morgenstern, and A. Niehaus, Z. Phys. A **320**, 81 (1985).
[25]A. Wada, F. Koike, K. Wakiya, T. Takayanagi, and H. Suzuki, J. Phys. B **20**, 1261 (1987).
[26]P. v.d. Straten and R. Morgenstern, Comments At. Mol. Phys. D **17**, 243 (1986).
[27]R. B. Barker and H. W. Berry, Phys. Rev. **151**, 14 (1966).
[28]P. v.d. Straten and R. Morgenstern, J. Phys. B **19**, 1361 (1986).
[29]P. W. Arcuni, Phys. Rev. A **33**, 105 (1986).
[30]P. v.d. Straten and R. Morgenstern, Phys. Rev. A **34**, 4482 (1986).
[31]R. Morgenstern, A. Niehaus, and U. Thielmann, J. Phys. B **10**, 1039 (1977).
[32]P. v.d. Straten, R. Morgenstern, and A. Niehaus, J. Phys. B **21**, 1573 (1988).